AD-A076 154 NAVAL RESEARCH LAB WASHINGTON DC F/G 20/9
ELECTROMAGNETIC INSTABILITIES IN A FOCUSED ION BEAM PROPAGATING--ETC(U
OCT 79 P F OTTINGER , D MOSHER ES-77-A-01-6021
UNCLASSIFIED NRL-MR-4088 NL

1 OF 1
AD
A076154

END
DATE
FILMED
11-79
DDC

(12) LEVEL II

(14) NRL-MR-

NRL Memorandum Report 4088

(6)

Electromagnetic Instabilities in a Focused Ion Beam Propagating Through a z-Discharge Plasma

(10) P. F. Ottinger, D. Mosher and Shyke A. Goldstein

Plasma Physics Division

(9) Interim rept.,

(11) 15 October 1979

(12) 26

(15) ES-77-A-01-6921

NAVAL RESEARCH LABORATORY
Washington, D.C.

251950

SECURITY CLASSIFICATION OF THIS PAGE (When Data Entered)

REPORT DOCUMENTATION PAGE

READ INSTRUCTIONS BEFORE COMPLETING FORM

1. REPORT NUMBER: NRL Memorandum Report 4088
2. GOVT ACCESSION NO.
3. RECIPIENT'S CATALOG NUMBER

4. TITLE (and Subtitle): ELECTROMAGNETIC INSTABILITIES IN A FOCUSED ION BEAM PROPAGATING THROUGH A z-DISCHARGE PLASMA

5. TYPE OF REPORT & PERIOD COVERED: Interium report on a continuing NRL problem

6. PERFORMING ORG. REPORT NUMBER

7. AUTHOR(s): P. F. Ottinger[a], D. Mosher, and Shyke A. Goldstein[a]

8. CONTRACT OR GRANT NUMBER(s)

9. PERFORMING ORGANIZATION NAME AND ADDRESS: Naval Research Laboratory, Washington, D.C. 20375

10. PROGRAM ELEMENT, PROJECT, TASK AREA & WORK UNIT NUMBERS: ES-77-A-01-6021; NRL Problem: 67-H02-29B

11. CONTROLLING OFFICE NAME AND ADDRESS: Department of Energy, Washington, D.C. 20545

12. REPORT DATE: October 15, 1979

13. NUMBER OF PAGES: 25

14. MONITORING AGENCY NAME & ADDRESS (if different from Controlling Office)

15. SECURITY CLASS. (of this report): Unclassified

15a. DECLASSIFICATION/DOWNGRADING SCHEDULE

16. DISTRIBUTION STATEMENT (of this Report)

Approved for public release; distribution unlimited.

17. DISTRIBUTION STATEMENT (of the abstract entered in Block 20, if different from Report)

18. SUPPLEMENTARY NOTES

This research was supported by the Department of Energy project number 67-H02-29B.
a. Present address: JAYCOR, Alexandria, Virginia 22304.

19. KEY WORDS (Continue on reverse side if necessary and identify by block number)

Electromagnetic Instabilities
Ion Beam Propagation
Z-Discharge Plasma Channel
Ion Orbits

20. ABSTRACT (Continue on reverse side if necessary and identify by block number)

A beam-plasma system consisting of a focused light ion beam propagating through a z-discharge plasma is analyzed for electromagnetic velocity space instabilities. In particular, the Weibel ~~($\mathbf{k} \cdot \mathbf{B} = 0, \mathbf{k} \cdot \mathbf{V}_z \simeq 0$)~~ and the Whistler ~~($\mathbf{k} \times \mathbf{B} \simeq 0, \mathbf{k} \cdot \mathbf{V}_z = 0$)~~ instabilities are studied. It is found that unstable modes do not grow fast enough to affect the beam propagation in a pellet-fusion-reactor chamber. For $\mathbf{k} \cdot \mathbf{V}_z \gtrsim 0$, the instabilities convect with a velocity much less than the beam streaming velocity.

DD FORM 1 JAN 73 1473 EDITION OF 1 NOV 65 IS OBSOLETE
S/N 0102-014-6601

SECURITY CLASSIFICATION OF THIS PAGE (When Data Entered)

CONTENTS

ELECTROMAGNETIC INSTABILITIES IN A FOCUSED ION BEAM PROPAGATING THROUGH A z-DISCHARGE PLASMA

I. INTRODUCTION

In an earlier paper,[1] it was shown that focused ion beams for use in a pellet fusion device can propagate axially down a z-discharge plasma channel without generating disruptive microturbulence due to electrostatic streaming instabilities. The azimuthal magnetic field in the z-discharge channel confines the beam radially as it propagates. Here the analysis will be extended to study electromagnetic velocity-space instabilities. In particular, the Weibel instability ($\mathbf{k} \cdot \mathbf{B} = 0$, $\mathbf{k} \cdot \mathbf{V}_z \simeq 0$) and the Whistler instability ($\mathbf{k} \times \mathbf{B} \simeq 0$, $\mathbf{k} \cdot \mathbf{V}_z \simeq 0$) are investigated, where $\mathbf{k}$ is the wavevector, $\mathbf{B}$ is the azimuthal magnetic field and $\mathbf{V}_z = V_z \hat{e}_z$ is the axial streaming velocity of the beam.

The beam-plasma system consists of a focused ion beam (typically a 5 MeV proton beam of 50 ns duration, 0.5 cm radius, and a current of $5 \times 10^5 A$) propagating down the axis of a z-discharge plasma channel.[2] The ion beam is focused at the entrance to the plasma channel (see Figure 1) with velocity components transverse to z given by $V_\perp / V_z \simeq \tan\theta << 1$. A high plasma density in the channel ($n_p \approx 10^{18}\,\mathrm{cm}^{-3}$) insures good beam charge neutralization.[3] Good beam current neutralization in the interior of the beam also occurs, so that the total magnetic field is comparable to that associated with the preformed channel established before beam injection. The beam current greatly exceeds that establishing the channel so the electron drift velocity is approximated by $V_e \simeq n_b V_z / n_p$.

Manuscript submitted August 6, 1979.

Hydrodynamic modeling of the background plasma[4] shows that a uniform channel net-current model is appropriate for the early times associated with passage of the beam front. This is because the low-temperature channel is established microseconds before beam injection so that complete magnetic diffusion occurs. Later in the ion pulse, expansion of the beam-heated high-temperature plasma ($T \simeq$ 25-50 eV) reduces the magnetic field strength in the interior of the channel. The built-up field in the expanding cylindrical shock wave is also enhanced by significant current non-neutralization in the cool plasma surrounding the beam-heated channel. The maximum field strength just outside the ion-beam radius can exceed that established by the initial z-discharge current by a large factor. Thus, at late times during beam passage, the magnetic field distribution is closely approximated by a surface-current model.

In Sec. II, equilibrium models for such a beam plasma system will be described. In Secs. III and IV, the Wiebel and Whistler instabilities will be investigated. The conclusions which can be drawn from this work are summarized in Sec. V.

II. BEAM-PLASMA EQUILIBRIUM

For mathematical convenience, a slab model will be used for the beam-plasma system. This is appropriate for the case at hand since ions are injected into the channel with small angular momentum so that the resulting orbital motion occurs in a plane. At early times in the pulse, the net current (nearly equal to the channel current) is uniformly distributed across the channel and flows in the z direction. Thus, $\mathbf{B} = B_y \hat{e}_y$ where

$$B_y = \begin{cases} B_p x/a, & |x| < a \\ B_p, & |x| > a \end{cases} \tag{1}$$

Here, B_p is the peak value of the field and "a" is the channel radius. If the beam distribution function f_b is written as

$$f_b(v_x, v_y, v_z) = \frac{n_b}{\pi}\, \delta(v_y)\, \delta\left(v_x^2 + v_z^2 - \frac{2V_z P_z}{m_i} + K\right) \tag{2}$$

where $P_z = m_i v_z + eA_z/c$ is the axial canonical momentum, A_z is the vector potential and n_b, V_z and K are constants, then

$$n_b(x) = \begin{Bmatrix} n_b, & |x| < r_b \\ 0, & |x| > r_b \end{Bmatrix}, \tag{3}$$

where $r_b = V_\beta/\omega_o$, $K = V_z^2 - V_\beta^2$, $\omega_o^2 = V_z\bar{\omega}_{ci}/a$ and $\bar{\omega}_{ci} = eB_p/m_i c$. A smoothly falling density profile may be obtained by replacing the second delta function in Eq (2) by a Maxwellian distribution function. The distribution function in Eq. (2) also states that all beam ions cross the axis at the same angle and traverse the entire beam radius during each betatron oscillation. A more complicated distribution function could be used to model the small spread in angles at which the ions cross the axis, however little additional information is obtained for the effort. For mathematical convenience, the form of the distribution function given in Eq (2) will be used here. It is easy to show that the fluid velocity is given by $\mathbf{V} = V_z\hat{\mathbf{e}}_z$ and that in order for the beam to be confined within the plasma channel, one must have $r_b \leqslant a$. Furthermore, f_b can be written in the more convenient form

$$f_b(v_y, v_\beta, \phi) = \frac{n_b}{\pi}\,\delta(v_y)\,\delta(v_\beta^2 - V_\beta^2 + \omega_o^2 x^2), \tag{4}$$

where $v_x \equiv v_\beta \sin\phi$, $v_z \equiv V_z + v_\beta \cos\phi$ and $v_\beta^2 = v_x^2 + (v_z - V_z)^2$. Here, V_z is associated with the average streaming velocity of the beam ions and v_β is associated with the oscillatory betatron motion of the beam ions ($v_\beta \leqslant V_\beta = \omega_o r_b$). The beam-ion orbit equations for this field geometry were solved in Ref. 1 and the results are summarized in Appendix A.

The distribution function given in Eqs. (2) or (4) provides an appropriate discription of the ion beam at early times in the pulse. At late times $B_y = 0$ inside the channel and the field is built-up sharply at the radial edge of the beam. Thus at late times in the pulse

$$f_b(v_y, v_\beta, \phi) = \begin{Bmatrix} \frac{n_b}{\pi}\,\delta(v_y)\,\delta(v_\beta^2 - V_\beta^2), & |x| < r_b \\ 0, & |x| > r_b + \delta \end{Bmatrix}, \tag{5}$$

where $B_y(r_b + \delta)$ is sufficiently large to confine the beam and the sheath is restricted to a thin layer such that $\delta << r_b$. Beam ions move in straight line orbits inside the field-free channel. Within the layer $\gamma_b < |x| \leqslant \gamma_b + \delta$, the ions reflect off the magnetic wall, reverse their transverse velocity and resume their straight line trajectories after reentering the channel. The distribution function in Eq. (5) also results in the uniform density profile of Eq. (3) and in a fluid velocity given by $\mathbf{V} = V_z\hat{e}_z$ inside the channel.

The background plasma provides complete charge and nearly complete current neutralization of the beam. In addition, the plasma also carries the z-discharge current. The high density desired for good beam neutralization provides for a high frequency of electron-plasma ion collisions, ν_e, shown[4] to be larger than ω_{ce} inside the channel at all times during the pulse. Thus, a collisional fluid model is used for the background plasma with the electrons drifting with velocity $\mathbf{V}_e \simeq (n_b V_z/n_p)\,\hat{e}_z$.

III. THE WEIBEL INSTABILITY

Two Weibel instabilities will be investigated, the ion instability and the electron instability, which are respectively driven by the streaming of the beam ions and the electron drift motion. Lee and Lampe[5] report for electron beams that the Weibel instability grows at a greatly reduced rate when $V_\perp/V_z > \omega_{pb}/\omega_{pe}$ where ω_{pb} is the beam plasma frequency and ω_{pe} is the electron plasma frequency. Molvig[6] has shown that is possible for electron-ion colisions to restore rapid growth of the mode. Although the concern here is with ion beams driving the instability, again both beam-thermal effects and collisional effects are important. Ion betatron motion will also be important in analyzing the ion instability.

A. Ion Instability

Consider first the situation late in the beam pulse, with f_b given by Eq. (5). For assumed large r_b, the perturbed distribution function with $\mathbf{E}(\mathbf{x}) = \mathbf{E}\exp(ikx)$,

$$f_{b1} = \frac{-e}{m_i}\int_{-\infty}^{0} d\tau\left[\mathbf{E} + \frac{\mathbf{v}\times\mathbf{B}}{c}\right]\cdot\frac{\partial f_b}{\partial \mathbf{v}}\exp i(k\mathrm{v}_x - \omega)\,\tau, \tag{6}$$

can be integrated over τ to give

$$f_{b1} = \left(\frac{-ie/m_i}{\omega - k\mathrm{v}_x}\right)\left[\left(E_x + \frac{k\mathrm{v}_z}{\omega}E_z\right)\frac{\partial f_b}{\partial \mathrm{v}_x} + \left(1 - \frac{k\mathrm{v}_x}{\omega}\right)E_z\frac{\partial f_b}{\partial \mathrm{v}_z}\right]. \tag{7}$$

Here $\mathbf{k} = k\hat{e}_x$ and straight-line unperturbed orbits are used since $B_y = 0$ for $|x| < r_b$. The assumption that $n_b/n_p << 1$ allows one to write the usual approximate dispersion equation,[6] $D_{zz} \approx 0$, for the Weibel instability where $|\omega| < \nu_e$ and

$$D_{zz} \approx 0 = c^2k^2 + \gamma^2 + \omega_{pi}^2\gamma/\nu_i + I_{zz}. \tag{8}$$

Here $\omega = i\gamma$ for purely growing perturbations,[6] $\nu_i = m_e\nu_e/m_i$, $V_z >> V_e$ (electron drift motion is ignored at present) and I_{zz} is the beam contribution to D_{zz};

$$I_{zz} = \frac{-4\pi e^2}{m_i}\int\left[\left(\frac{k\mathrm{v}_z^2}{i\gamma - k\mathrm{v}_x}\right)\frac{\partial f_b}{\partial \mathrm{v}_x} + \mathrm{v}_z\frac{\partial f_b}{\partial \mathrm{v}_z}\right]d^3\mathrm{v}. \tag{9}$$

Integrating by parts and then using the calculus of residues to perform the remaining nontrivial integration results in

$$I_{zz} = \frac{\omega_{pb}^2\gamma}{k^2V_\beta^2}\left[\frac{k(V_\beta + 2V_z)}{(1 + \gamma^2/k^2V_\beta^2)^{1/2}} - \frac{2k^2V_zV_\beta}{\gamma} - \frac{kV_z^2/V_\beta}{(1 + \gamma^2/k^2V_\beta^2)^{3/2}}\right] \tag{10}$$

which reduces to

$$I_{zz} = \begin{cases} -\omega_{pb}^2\left(\dfrac{2V_z}{V_\beta} + \dfrac{V_z^2\gamma}{kV_\beta^3}\right), & \gamma << kV_\beta \\ -\omega_{pb}^2\left(1 - \dfrac{k^2V_z^2}{\gamma^2}\right), & \gamma >> kV_\beta \end{cases}, \tag{11}$$

for $V_z > V_\beta$ and the limits shown. Solving Eq. (8) for the growth rate, γ, one obtains

$$\gamma = \begin{cases} (k^2 V_z^2 \nu_i \omega_{pb}^2/\omega_{pi}^2)^{1/3}, & 0 < k < k_p \\ \left(\dfrac{2\omega_{pb}^2 \nu_i V_z}{\omega_{pi}^2 V_\beta}\right)\left(1 + \dfrac{2\omega_{pb}^2 V_z^2 \nu_i}{\omega_{pi}^2 k V_\beta^3}\right), & k_p < k < k_o \\ 2\omega_{pb} c (2V_z/V_\beta)^{1/2} (k_o - k), & k \simeq k_o \end{cases}, \tag{12}$$

where

$$k_p = (\omega_{pb}^2 \nu_i V_z^2/2^{3/2}\omega_{pi}^2 V_\beta^3); \quad k_o = (\omega_{pb}/c)\ (2V_z/V_\beta)^{1/2}.$$

The peak growth rate is given by

$$\gamma_p' = \frac{\omega_{pb}^2 \nu_i}{\omega_{pi}^2}\left(\frac{2V_z^2}{V_\beta^2}\right)^{4/5} \quad \text{at} \quad k = k_p. \tag{13}$$

For $n_b/n_p \sim 10^{-3}$ and $V_\beta/V_z \gtrsim 10^{-1}$, $\gamma_p' \sim 10^6$ sec^{-1} at late times in the beam pulse (note that γ_p' is actually overestimated here since $k_p r_b << 1$). Thus, no significant growth can occur since $\gamma_p' \tau_b \gtrsim 0.05$; here τ_b is the beam pulse length.

At early times in the beam pulse, ν_i is larger due to low channel temperatures so that one might expect the growth rate to be larger. It will be found, however, that by including the betatron motion of beam ions in the analysis, the perturbation is stabilized. In this case, f_b is given by Eq. (4), the ion orbits are found in Appendix A, and f_{b1} is given by

$$f_{b1} = \frac{-2e}{m_i}\frac{\partial f_b}{\partial v_\beta^2}\int_{-\infty}^{0} d\tau \Big[v_x' E_x(x') + (v_z' - V_z)\ E_z(x') \Big[-\frac{iV_z v_x'}{\omega}\frac{\partial E_z}{\partial x'}\Big] \exp(i\omega\tau) \tag{14}$$

It is now assumed that $E_z(x) \simeq \bar{E}_z \cos kx$ where k is restricted to a discrete set of values by boundary conditions at r_b with $kr_b \gtrsim 1$. This choice of $E_z(x)$ is reasonble since n_p and n_b are both uniform and $n_b << n_p$. Thus, the mode is expected to closely resemble the background plasma eigenmode which is sinusoidal. Here again, the background plasma is treated as

a collisional fluid since $\nu_e > \omega_{ce}$. An approximate algebraic dispersion equation is obtained by taking a weighted spatial average of $\hat{D}_{zz}E_z(x)$ where $\hat{D}_{zz}$ is a differential operator in x defined by

$$\hat{D}_{zz} = -c^2\frac{\partial^2}{\partial x^2} + \gamma^2 + \frac{\omega_{pi}^2\gamma}{\nu_i} - 4\pi ie \int v_z f_{b1} d^3v$$

and f_{b1} is given in Eq. (14) ($E_x \approx 0$). The dispersion equation is then

$$0 \approx \bar{D}_{zz} \equiv \frac{1}{r_b \bar{E}_z} \int_{-r_b}^{r_b} dx\ \hat{D}_{zz}E_z(x) \cos kx \tag{15}$$

Using the orbit equations for $\mathbf{x}'$ and $\mathbf{v}'$ found in Appendix A and the Bessel function identities

$$\exp(\pm\ iz \sin\theta) = J_o(z) + 2\sum_{l=1}^{\infty} J_{2l}(z) \cos 2l\theta$$

$$\pm\ 2i \sum_{l=0}^{\infty} J_{2l+1}(z) \sin\ (2l+1)\ \theta, \tag{16}$$

and

$$\exp(iz \cos\theta) = J_o(z) + 2\sum_{l=1}^{\infty} i^l J_l(z) \cos l\theta, \tag{17}$$

the τ integration in Eq. (14) can be performed. Thus, Eq. (15) takes the form

$$0 = c^2k^2 + \gamma^2 + \frac{\omega_{pi}^2\gamma}{\nu_i} + \bar{I}_{zz} \tag{18}$$

where in terms of $\alpha_1(x, v_x, v_z)$ and $\alpha_2(x, v_x, v_z)$

$$\bar{I}_{zz} = \frac{-2\omega_{pb}^2}{n_b} \int_{-r_b}^{r_b} dx \cos kx \int d^3v\ v_z \frac{\partial f_b}{\partial v_\beta^2} \left[\frac{kV_z}{\gamma}\ \alpha_1 + \alpha_2\right]. \tag{19}$$

The expressions for α_1 and α_2 are given in Appendix B. Terms involving resonances at higher harmonics of ω_o [i.e. $(\omega - m\omega_o)^{-1}$ for $m \neq 0$] are not considered. The term involving α_1 in Eq. (19) is the source of instability. Here, however, because of the betatron motion, this term vanishes and the mode is stable at early times in the pulse (see Appendix B). This same result is obtained for odd eigenfunctions, $E_z(x) = \bar{E}_z \sin kx$. Mathematically the term vanishes because the integrand involving α_1 is an odd function of x (see Appendix B). Physically no

radial current bunching can occur since each ion travels radially back and forth across the beam profile as it follows its betatron orbit. However, azimuthal current bunching can occur as will be discussed in Sec. IV.

B. Electron Instability

The only other source of energy available to drive the Weibel instability at early times in the pulse is the drifting electron background. The drift velocity, however, is actually subthermal since even before beam heating occurs $V_e \simeq n_b V_z/n_p < u_e = (T/m_e)^{1/2}$. Using a warm collisional model ($\nu_e > \omega_{ce}$ at all times), the dispersion equation for the electron-Weibel instability is derived in Appendix C. Setting $\gamma = 0$ in Eq. (C7), it is found that $\gamma > 0$ for $0 < k < k_o = \omega_{pi} V_e/\sqrt{2} u_i c$, where $u_i = (T/m_i)^{1/2}$. Thus for $k < k_o$ and $\omega_{pi}^2 > \gamma\nu_i$, Eq. (C8) reduces to

$$0 = c^2k^2 + \frac{\omega_{pi}^2\gamma}{\nu_i} - \frac{\omega_{pi}^2 k^2 V_e^2(\gamma^2 + \nu_i\gamma + k^2u_i^2)}{(\gamma^4 + \nu_i\gamma^3 + 3k^2u_i^2\gamma^2 + 2\nu_i k^2u_i^2\gamma + 2k^4u_i^4)}, \tag{20}$$

where the ion beam contribution to Eq. (20) is ignorable.

At early times in the pulse, $\omega_{pi}u_i/c\nu_i < 1$ and

$$\gamma = \begin{cases} (k^2V_e^2\nu_i)^{1/3}, & 0 < k < \tilde{k}_1 \\ \omega_{pi}V_e/c, & \tilde{k}_1 < k < k_o \\ \dfrac{\sqrt{2}\,\nu_i c V_e}{\omega_{pi}u_i}\,(k_o - k), & k \approx k_o \end{cases}, \tag{21}$$

where $\tilde{k}_1 = (\omega_{pi}/c)\,(\omega_{pi}V_e/c\nu_i)^{1/2}$. Here $T \approx 4$ eV, $n_p \simeq 2 \times 10^{18}$ cm^{-3} and $n_b/n_p \simeq 5\times10^{-4}$, so that the peak growth rate is on the order of $\gamma_p = \omega_{pi}V_e/c = 4.2\tau_b^{-1}$.

At later times in the pulse, the beam has heated the plasma; then $\omega_{pi}u_i/c\nu_i > 1$ and

$$\gamma = \begin{cases} (k^2V_e^2\nu_i)^{1/3}, & 0 < k < k_1 \\ V_e^2\nu_i/2u_i^2, & k_1 < k < k_2 \\ \dfrac{kV_e}{2}\left[1 - \dfrac{2k^2c^2u_i^2}{\omega_{pi}^2V_e^2}\right]^{1/2}, & k_2 < k \leqslant k_o \end{cases}, \tag{22}$$

where $k_1 = \nu_i V_e^2/u_i^3$, $k_2 = \nu_i V_e/u_i^2$ and $V_e \lesssim u_i$. Now $\gamma_p^e = \omega_{pi} V_e^2/(2^{3/2} c u_i) \simeq 1.0\tau_b^{-1}$ for $T \simeq 38$ eV, $n_p \sim 1 \times 10^{18}$ cm^{-3} and $n_b/n_p \sim 1 \times 10^{-3}$. Thus, $\gamma_p^e \tau_b$ decreases by a factor of four as the beam passes through and heats the plasma. In fact, $\omega_{pi} u_i/c\nu_i = 1$ at $t \approx 10.0$ ns into the pulse so that a total of about 1.6 e-folds occur during the transit of the beam.

Note that τ_b is the appropriate time scale for instability growth since $V_e = 0$ except during the passage of the beam. Furthermore, for small k_z (i.e. $k_z^2 < 2\omega_{pi}^2/3c^2$), it can be shown from Eq. (C9) that

$$v_g = \frac{\partial \omega_r}{\partial k_z} = \frac{3k_z^2 V_e^3}{2\gamma_o^2} < V_e << V_z, \tag{23}$$

and

$$\gamma = \gamma_o - \frac{k_z^2 V_e^2}{2\gamma_o}, \tag{24}$$

where $\gamma_o = \omega_{pi} V_{e/c}$. Thus, the unstable mode convects axially, but with a group velocity, v_g, which is much slower than V_z or V_e. At any given point in the plasma the mode grows only for a time of order τ_b. For larger k_z and fixed k_x the mode transforms into the electrostatic streaming instability which was found to be stable in Ref. 1.

C. Summary for the Weibel Instabilities

In summary, it is found that the betatron motion of the beam ions stabilizes the ion-Weibel instability at the beam front while growth is too slow at the tail of the beam to allow for even one e-fold ($\gamma_p^i \tau_b \gtrsim 0.05$). The electron-Weiber instability, on the otherhand, grows fastest ($\gamma_p^e \tau_b \simeq 4.2$) at the front of the beam where the plasma is relatively cold. At the tail of the beam $\gamma_p^e \tau_b \simeq 1.0$. Although the electron-Weibel instability grows faster than the ion-Weibel instability, it also is not expected to grow to a level which could seriously affect beam propagation.

IV. THE WHISTLER INSTABILITY

The Whistler mode ($\mathbf{k} \times \mathbf{B} \simeq 0$, $\mathbf{k} \cdot \mathbf{V}_z = 0$) like the Weibel instability can be driven unstable by particle streaming. However, the wavevector $\mathbf{k} = k_y \hat{e}_y$ (i.e. $\hat{e}_o$ in cylindrical geometry) is perpendicular to the direction of the betatron motion of the beam ions. Hence, unlike the Weibel instability, the Whistler instability cannot be stabilized by the beam ion betatron motion. However, a small spread in v_y (angular momemtum) can reduce the growth rate significantly. The electron drift velocity is ignored when considering the ion-Whistler instability since $V_z >> V_e$.

Consider first the situation late in the beam pulse with f_b given by Eq. (5). If it is assumed for the moment that r_b is very large, then the perturbed distribution function is given by

$$f_{b1} = \left[\frac{-ie}{m_i}\left(\mathbf{E} + \frac{\mathbf{v} \times \mathbf{B}}{c}\right) \cdot \frac{\partial f_b}{\partial \mathbf{v}}\right] / (\omega - k_y v_y). \tag{25}$$

Using this expression for f_{b1}, the perturbed current is easily calculated and used to derive the dispersion equation,

$$D_{zz} = c^2 k^2 y + \gamma^2 + \frac{\omega_{pi}^2 \gamma}{\nu_i} + \omega_{pb}^2 \left\{1 - \frac{k^2 (V_z^2 + V_\beta^2/2)}{\gamma^2}\right\} \simeq 0. \tag{26}$$

Again $n_b/n_p << 1$ was used in deriving Eq. (26) where $\omega = i\gamma$ for purely growing perturbations and $V_e << V_z$ (electron drift motion is ignored at present).

Solving Eq. (26) yields

$$\gamma = \begin{Bmatrix} k_y V_z, & 0 < k_y < k_1 \\ (k_y^2 V_z^2 \omega_{pb}^2 \nu_i / \omega_{pi}^2)^{1/3}, & k_1 < k_y < k_2 \\ \omega_{pb} V_z / c, & k_y > k_2 \end{Bmatrix}, \tag{27}$$

where

$$V_z > V_\beta;\ k_1 = \omega_{pb}^2 \nu_i / \omega_{pi}^2 V_z;\ \ k_2 = (\omega_{pi}/c)\ (\omega_{pb} V_z / \nu_i c)^{1/2}.$$

The peak growth rate (for $k_y > k_2 \simeq 25.0\ \text{cm}^{-1}$) is given by $\gamma_p' = \omega_{pb} V_z/c \simeq 2 \times 10^2\, \tau_b^{-1}$, for a beam with no spread in v_y.

This result is only slightly modified when finite geometry effects and the betatron motion of the beam ions and included. Proceeding as in Appendix B with $\mathbf{k} = k_x\hat{\mathbf{e}}_x + k_y\hat{\mathbf{e}}_y$ and f_b given in Eq. (4), one obtains

$$D_{zz} = c^2(k_x^2 + k_y^2) + \gamma^2 + \frac{\omega_{pi}^2\gamma}{\nu_i} + \omega_{pb}^2\left[F(k_x r_b) - \frac{k_y^2(V_z^2 + V_\beta^2/2)}{\gamma^2}\, G(k_x r_b)\right], \tag{28}$$

where $F(k_x r_b)$ is defined in Eq. (B6). The quantity $G(k_x r_b)$ is defined by

$$G(k_x r_b) \equiv \frac{2}{k_x N}\int_o^{k_x r_b} \cos X\Big[J_o(X)\, J_o^2(Z) + 2\sum_{n=1}^{\infty} J_{2n}(X)\, J_n^2(Z)\Big]_{Z=\tilde{Z}(X)}, dX \tag{29}$$

with $X = k_x x$, $\tilde{Z}(X) = (k_x r_b/2)\,(1 - X^2/k_x^2 r_b^2)^{1/2}$ and $N = r_b + (\sin 2k_x r_b)/2k_x$. Note that $G(k_x \simeq 0) = 1$. F and G are only geometrical factors and do not modify the structure of the dispersion equation. For large k_y the peak growth rate now becomes $\gamma_p' = (\omega_{pb} V_z/c)\,[G(k_x r_b)]^{1/2}$, which, aside from the geometrical correction, is identical to γ_p found in Eq. (27).

If the beam has a small spread in v_y, the beam can be modeled by the distribution function

$$f_b = \frac{n_b}{\pi^{3/2} V_y}\,\delta(v_\beta^2 - V_\beta^2)\,\exp(-v_y^2/V_y^2), \tag{30}$$

where V_y is the thermal velocity of the beam ions. Since the y motion is unaffected by B_y, the distribution in v_y will be the same at all points inside the channel. For convenience finite geometry effects and the effects of the betatron motion of the beam ions are ignored here since they have little affect on the Whistler mode. Substituting the distribution function of Eq. (30) into Eq. (25) yields an expression for the perturbed distribution function, f_{b1}. The perturbed current j_{b1} can then be calculated and the dispersion equation derived.

$$D_{zz} = c^2k^2 + \gamma^2 + \omega_{pi}^2\gamma/\nu_i + I_{zz} \simeq 0. \tag{31}$$

In Eq. (31), $\omega = i\gamma$ and

$$I_{zz} = \frac{\omega_{pb}^2}{\sqrt{\pi}V_y}\int_{-\infty}^{\infty} dv_y\left[1 + \frac{2k_y v_y(V_z^2 + V_\beta^2/2)}{V_y^2(i\gamma - k_y v_y)}\right]\exp(-v_y^2/V_y^2). \tag{32}$$

Here, the v_β and ϕ integrations are trivial and have already been carried out. The quantity I_{zz} is easily written in terms of the usual plasma dispersion function, $Z(\zeta)$[8]. However, here ζ is pure imaginary so that

$$I_{zz} = \omega_{pb}^2\left\{1 - \frac{2V_z^2}{V_y^2}\left[1 - \frac{\sqrt{\pi}\gamma}{k_y V_y}\exp\left(\frac{\gamma^2}{k_y^2V_y^2}\right)\left[1 - erf\left(\frac{\gamma}{k_y V_y}\right)\right]\right]\right\}, \tag{33}$$

where $V_z > V_\beta$ and $erf(x)$ is the usual error function.[9] For $\gamma > kV_y$, Eq. (31) reduces to Eq. (26), but for $\gamma < kV_y$ the dispersion equation becomes

$$0 = c^2k^2 + \gamma^2 + \frac{\omega_{pi}^2\gamma}{\nu_i} + \omega_{pb}^2\left[1 - \frac{2V_z^2}{V_y^2}\left[1 - \frac{\sqrt{\pi}\gamma}{kV_y} + \frac{2\gamma^2}{k^2V_y^2} + \cdots\right]\right]. \tag{34}$$

From this it is found that the peak growth rate, $\gamma_p = \omega_{pb}V_z/c$, for the case with $V_y = 0$ is reduced if $V_y^2 > 2\nu_i\omega_{pb}cV_z/\omega_{pi}^2$. Since this is the case here

$$\gamma = \begin{cases} kV_z, & 0 < k < k_1 \\ (k^2V_z^2\nu_i\omega_{pb}^2/\omega_{pi}^2)^{1/3}, & k_1 < k < k_2 \\ \dfrac{2\omega_{pb}^2\nu_i V_z^2}{\omega_{pi}^2V_y^2}\left[1 - \dfrac{c^2k^2V_y^2}{2\omega_{pb}^2V_z^2}\right], & k_2 < k \leqslant k_o \end{cases}, \tag{35}$$

where $k_1 = \omega_{pb}^2\nu_i/\omega_{pi}^2V_z$, $k_2 = k_1V_z^2/V_y^2$ and $k_o = \sqrt{2}\,\omega_{pb}V_z/cV_y$.

The peak growth rate is now

$$\gamma_p' = (\omega_{pb}V_z/c)\,(2\nu_i\omega_{pb}cV_z/V_y^2\omega_{pi}^2) < \omega_{pb}V_z/c,$$

where γ_p' varies in time as $T^{-3/2}(t)$ through ν_i. The number of e-folds, δ during the beam transit at any point in the plasma is given by

$$\delta = \int_0^{\tau_b}\gamma_p'(t)\,dt = \gamma_p'(0)\int_0^{\tau_b}\frac{dt}{(1 + \Delta Tt/\tau_b)^{3/2}}. \tag{36}$$

where it is demonstrated later than no significant wave convection occurs. Here $\Delta T = [T(\tau_b) - T(0)]/T(0)$ for T in eV and $\gamma_p'(0)$ is the peak growth rate at the front of the beam. A linear rise in temperature, $T(t)/T(0) = 1 + \Delta T t/\tau_b$, agrees well with results of previous work.[3] Thus

$$\delta = \frac{2\gamma_p'(0)\,\tau_b}{\Delta T}\left[1 - \frac{1}{(1+\Delta T)^{1/2}}\right] \tag{37}$$

For $T(\tau_b)$ 40 eV, $T(0) = 4$ eV, $\tau_b = 50$ ns, $V_y/V_z \gtrsim 0.08$ and $n_b/n_p = 10^{-3}$, $\delta \lesssim 1.0$ e-folds. A spread in V_y then reduces the growth of the ion-Whistler instability to a tolerable level.

Finally it can also be shown that the ion-Whistler instability does not convect with the beam when $k_z \gtrsim 0$. This needs to be verified in order to justify using τ_b as the appropriate time scale. Taking Eq. (5) for f_b and setting $k = k_y\hat{e}_y + k_z\hat{e}_z$ this dispersion equation becomes

$$0 = c^2k_y^2 - (\omega_r + i\gamma)^2 + \frac{\omega_{pi}^2}{\nu_i}(\omega_r + i\gamma) + I_{zz}, \tag{38}$$

where $\omega = \omega_r + i\gamma$ and

$$I_{zz} = \frac{\omega_{pb}^2}{2\pi}\int_0^{2\pi} d\phi\left[\frac{\omega^2 + k_y^2(V_z^2 + 2V_zV_\beta\cos\phi + V_\beta^2\cos^2\phi)}{(\omega - k_zV_z - k_zV_\beta\cos\phi)^2}\right] \tag{39}$$

Here the spread in v_y is neglected since it will have little effect on the axial group velocity of the perturbation. For mathematical convenience finite geometry effects and the betatron motion of the beam ions are also ignored. The results of the present calculation is actually an upper limit on the group velocity since the betatron motion of the beam ions will tend to wash out any disturbance moving axially on the beam. For $|\omega_r - k_zV_z| > k_zV_\beta$ the denominator of the integrand in Eq. (39) can be expanded and the integration is trivial. However, if $|\omega_r - k_2V_z| \lesssim k_zV_\beta$ the integration is most easily done using the calculus of residues. For small k_z and $V_\beta < V_z$, $|\omega_r - k_zV_z| > k_zV_\beta$ is appropriate for the ion-Whistler instability. Then integrating Eq. (39), Eq. (38) can be solved for ω_r and γ yielding

$$\gamma = \frac{\omega_{pb}}{c}(V_z^2 + V_\beta^2/2)^{1/2} - k_z V_z, \tag{40}$$

$$\omega_r = \frac{3}{2}\, k_z^2 V_z c/\omega_{pb}. \tag{41}$$

Clearly, $v_g = \partial\omega_r/\partial k_z < V_z$ for $k_z < \omega_{pb}/3c$. Thus the ion-Whistler instability does convect in the axial direction for $k_z < \omega_{pb}/3c$, but with a group velocity slower than the beam streaming velocity. For $k_z > \omega_{pb}/3c$ the calculus of residues can be used to evaluate Eq. (39), however, the mode is then basically an electrostatic two stream mode. This mode has already been shown to be stable in Ref. 1.

In summary it is found that, as expected, the betatron motion of the beam ions does not affect the ion-Whistler instability. The peak growth rate, however, can be reduced to a tolerable level by the presence of a spread in v_y (angular momentum in cylindrical geometry). The spread in v_y known to be present at injection in typical experiments[2] is sufficient to reduce the number of e-folds to less than 1.0. Furthermore, the mode convects axially at a group velocity less than V_z. The electron-Whistler instability was not considered, since it will have properties similar to the properties of the electron-Weibel instability (discussed in Section II.B) for such a highly collisional plasma ($\nu_e > \omega_{ce}$).

V. CONCLUSIONS

The purpose of this paper was to study electromagnetic velocity-space instabilities generated by a focused ion beam propagating through a z-discharge plasma. In particular, the Weibel instability ($\mathbf{k} \cdot \mathbf{B} = 0$, $\mathbf{k} \cdot \mathbf{V}_z \approx 0$) and the Whistler instability ($\mathbf{k} \times \mathbf{B} \approx 0$, $\mathbf{k} \cdot \mathbf{V}_z \approx 0$) were investigated. This work is an extension of the work in Ref. 1, where electrostatic instabilities were investigated.

The ion-Weibel instability (driven by the streaming energy of the beam ions) is found to be stabilized by the betatron motion of the beam ions at the front of the beam. At the tail of

the beam, where beam ions follow straight line orbits, the growth of the ion-Weibel instability is two slow to allow for even one e-fold ($\gamma_p^b \tau_b \approx 0.05$) during the transit of the beam. The electron-Weibel instability (driven by the drifting plasma electrons), on the other hand, grows fastest ($\gamma_p^e \tau_b \approx 4.2$) at the front of the beam where the plasma is relatively cold ($T \simeq 4$ eV). At the tail of the beam, where T rises to about 25-50 eV, $\gamma_p^e \tau_b \approx 1.0$. Although the electron-Weibel instability grows faster than the ion-Weibel instability, it also is not expected to grow to a level which could drastically affect beam propagation. Only 1.6 e-folds will occur during the transit of the beam. It has also been shown for $0 < k_z^2 < 2\omega_{pi}^2/3c^2$, where $\mathbf{k} = k_x\hat{\mathbf{e}}_x + k_z\hat{\mathbf{e}}_z$, that the electron-Weibel instability does convect axially but at a group velocity much less than the beam velocity ($v_g = 3k_z^2c^2V_e/2\omega_{pi}^2 < V_e << V_z$). Thus the appropriate growth period for calculating the number of e-folds is just the beam transit time, τ_b, and growth occurs mostly at the tail of the beam.

Because the plasma is highly collisional ($\nu_c > \omega_{ce}$ at all times), the electron-Whistler instability will have properties similar to those of the electron-Weibel instability. Thus it is also not expected to grow to a level which could drastically affect beam propagation.

The ion-Whistler instability, as expected, is not stabilized by the betatron motion of the beam ions. The peak growth rate, however, can be reduced to a tolerable level by the presence of a spread in v_y (angular momentum in cylindrical geometry). Furthermore, for $k_z < \omega_{pb}/3c$ the mode also convects axially at a group velocity less than V_z($v_g = 3k_zcV_z/\omega_{pb}$). Thus τ_b is again the correct time scale and only 1.0 e-fold are expected to occur during the transit of the beam in typical experiments.

From these results and from the results for electrostatic instabilities in Ref. 1, it can be concluded that it is possible to propagate a focused ion beam, appropriate for a pellet fusion

device, through a z-discharge plasma channel without generating significant growth of microinstabilities.

ACKNOWLEDGMENTS

This work was supported by U. S. Department of Energy.

APPENDIX A

For the magnetic field configuration given in Eq. (1) for $|x| < a$ the beam ion orbit equations were solved in paper I. The resulting ion orbits are given below:

$$x' = x \cos \omega_o \tau + \frac{v_x}{\omega_o} \sin \omega_o \tau, \tag{A1}$$

$$y' = y + v_y \tau \tag{A2}$$

$$z' = z + \left[v_z + \frac{\omega_o^2}{4 V_z} \left(\frac{v_x^2}{\omega_o^2} - x^2 \right) \right] \tau + \frac{\omega_o}{8 V_z} \left(x^2 - \frac{v_x^2}{\omega_o^2} \right) \sin 2\omega_o \tau - \frac{x v_x}{4 V_z} (\cos 2\omega_o \tau - 1), \tag{A3}$$

and

$$v_x' = v_x \cos \omega_o \tau - x \omega_o \sin \omega_o \tau, \tag{A4}$$

$$v_y' = v_y, \tag{A5}$$

$$v_z' = v_z - \frac{\omega_o^2}{4 V_z} \left(\frac{v_x^2}{\omega_o^2} - x^2 \right) (\cos 2\omega_o \tau - 1) + \frac{\omega_o x v_x}{2 V_z} \sin 2\omega_o \tau, \tag{A6}$$

where ω_o and V_z are the same as defined in Section II.

APPENDIX B

The expression for α_1 and α_2 found in Eq. (19) are

$$\alpha_1 = \frac{1}{N}\left\{v_x J_1(X)\left[\frac{1}{2}\,J_o(Y) + J_2(Y)\right] - x\omega_o J_1(Y)\left[\frac{1}{2}\,J_o(X) + J_2(X)\right]\right\}, \tag{B1}$$

$$\begin{aligned}\alpha_2 = \frac{1}{N}\Bigg\{&(v_z - V_z)\left[\frac{1}{2}\,J_o(X)\,J_o(Y) + 2\sum_{n=1}^{\infty}(-1)^n J_{2n}(X)\,J_{2n}(Y)\right] \\ &+ \frac{\omega_o^2}{8V_z}\left[\frac{v_x^2}{\omega_o^2} - x^2\right]\Bigg[J_o(X)\,J_o(Y) - 2J_o(X)\,J_2(Y) \\ &+ 2J_o(Y)\,J_2(X) + 4\sum_{n=1}^{\infty}(-1)^n\left[J_{2n}(X)\,J'_{2n+1}(Y) + \frac{2n+1}{X}\,J_{2n}(Y)\,J'_{2n+1}(X)\right]\Bigg] \\ &- \frac{\omega_o x v_x}{2V_z}\left[J_1(X)\,J_1(Y) + \sum_{n=1}^{\infty}(-1)^n\left[J_{2n+1}(X)\,J'_{2n-1}(Y) + J_{2n-1}(X)\,J_{2n+1}(Y)\right]\right]\Bigg\},\end{aligned} \tag{B2}$$

where $X = kx$, $Y = kv_x/\omega_o$ and $N = r_b + \sin 2kr_b/2k$.

In order to show that

$$I_1 = \frac{-2\omega_{pb}^2}{n_b}\int_{-r_b}^{r_b} dx\,\cos k_x \int d^3v\left[\frac{kV_z v_z}{\gamma}\,\frac{\partial f_b}{\partial v_\beta^2}\,\alpha_1\right] = 0, \tag{B3}$$

first write $v_x = v_\beta \sin\phi$ and $v_z = V_z + v_\beta\cos\phi$ and then perform the v_y and ϕ integration yielding

$$\begin{aligned}I_1 = \frac{-\omega_{pb}^2 k V_z^2}{\gamma N}\int_{-r_b}^{r_b} dx\,\cos kx \int dv_\beta^2\Bigg\{&\frac{\partial\delta(v_\beta^2 - V_\beta^2 + \omega_o^2 x^2)}{\partial v_\beta^2} \\ &\times\left[v_\beta J_1(X)\left[\frac{1}{2}\,J_{-1/2}(Z) + J_{3/2}(Z)\right]J_{1/2}(Z)\right. \\ &\left. - x\omega_o J_{1/2}^2(Z)\left[\frac{1}{2}J_o(X) + J_o(X)\right]\right]\Bigg\},\end{aligned} \tag{B4}$$

where $Z = k v_\beta / 2\omega_o$. Integrating by parts in v_β to remove the derivative of the delta function and then performing the v_β integration results in

$$I_1 = \frac{\omega_{pb}^2 k V_z^2}{4\gamma N \omega_o} \int_{-kr_b}^{kr_b} dX \cos X \left\{ \frac{J_1(X)}{Z} \left[\frac{1}{2} J_{-1/2}(Z) + J_{3/2}(Z) \right] J_{1/2}(Z) \right.$$
$$+ J_1(X) \left[\frac{1}{2} J'_{-1/2}(Z)\, J_{1/2}(Z) + \frac{1}{2} J_{-1/2}(Z)\, J'_{1/2}(Z) \right.$$
$$\left. + J'_{3/2}(Z)\, J_{1/2}(Z) + J_{3/2}(Z)\, J'_{1/2}(Z) \right]$$
$$\left. - \frac{X}{Z} J'_{1/2}(Z)\, J_{1/2}(Z) \left[\frac{1}{2} J_o(X) + J_2(X) \right] \right\}_{Z - \tilde{Z}(x)}, \tag{B5}$$

where $\tilde{Z}(x) = (kr_b/2)\,(1 - x^2/k^2 r_b^2)^{1/2}$. Since the integrand is an odd function of x, $I_1 = 0$.

The integral

$$I_2 = \frac{-2\omega_{pb}^2}{n_b} \int_{-r_b}^{r_b} dx \cos kx \int d^3v \left(v_z \alpha_2 \frac{\partial f_b}{2 v_\beta} \right) \equiv \omega_{pb}^2 F(kr_b) \tag{B6}$$

is more complicated and the associated term in the dispersion relation does not contribute to instability; hence it will suffice to write I_2 in terms of the function $F(kr_b)$ as defined in (B6).

APPENDIX C

For a warm collisional fluid, the continuity equation and momentum transport equations ($T_e \simeq T_i$ and $\nu_i = m_e\nu_e/m_i$) are

$$\frac{\partial n_\alpha}{\partial t} + \nabla \cdot (n_\alpha \mathbf{v}_\alpha) = 0, \tag{C1}$$

$$\frac{\partial \mathbf{v}_\alpha}{\partial t} + \mathbf{v}_\alpha \cdot \nabla \mathbf{v}_\alpha = \frac{q_\alpha}{m_\alpha}\left(\mathbf{E} + \frac{\mathbf{v}_\alpha \times \mathbf{B}}{c}\right) - \frac{T}{m_\alpha n_\alpha}\nabla n_\alpha - \nu_\alpha(\mathbf{v}_\alpha - \mathbf{v}_\beta), \tag{C2}$$

for $\alpha = i,e$. Linearizing Eqs. (C1) and (C2) for perturbations with exp $i(kx - \omega t)$ dependence and solving for the perturbed current results in

$$\mathbf{j}_e + \mathbf{j}_i = \frac{\omega_{pi}^2}{4\pi}\,\mathbf{I} \cdot \mathbf{E}, \tag{C3}$$

where

$$I_{xx} = \left(1 + \frac{\Omega_1^2}{\Omega_2^2}\right)/\Omega_3, \tag{C4}$$

$$I_{xz} = I_{zx} = -ikV_e\Omega_1/\gamma\Omega_2^2, \tag{C5}$$

$$I_{zz} = \frac{1}{\nu_i} - \frac{k^2V_e^2\Omega_3}{\gamma^2\Omega_2^2}, \tag{C6}$$

where $\omega = i\gamma$, $\Omega_1 = \gamma + k^2u_i^2/\gamma$, $\Omega_2^2 = \gamma\nu_i + k^2u_i^2 + 2\nu_ik^2u_i^2/\gamma + k^4u_i^4/\gamma^2$, and $\Omega_3 = \gamma + \nu_i + k^2u_i^2/\gamma$. In deriving expressions (C4)-(C6) it was assumed that $\gamma < \nu_e$.

Here the electron streaming is driving the instability and $n_e \approx n_i$ (unlike $n_b/n_e \ll 1$), thus the complete dispersion equation,

$$D_{xx}D_{zz} - D_{xz}D_{zx} = 0, \tag{C7}$$

must be used. This results in the following dispersion equation

$$0 = \left[\gamma^2 + \frac{\gamma\omega_{pi}^2}{\Omega_3}\left(1 + \frac{\Omega_1^2}{\Omega_2^2}\right)\right]\left[\gamma^2 + c^2k^2 + \frac{\gamma\omega_{pi}^2}{\nu_i} - \frac{\omega_{pi}^2k^2V_e^2\Omega_3}{\gamma\Omega_2^2}\right] + \frac{\omega_{pi}^4k^2V_e^2\Omega_1^2}{\Omega_2^4}. \tag{C8}$$

In order to study the axial convection of the electron Weibel instability, the dispersion equation must be rederived with $|k_z| \gtrsim 0$. For mathematical convenience thermal effects are ignored ($T = 0$ in Eq. (C2)). In this case, for large k_x, the dispersion equation is

$$0 = \left[c^2k_z^2 - \omega^2 - \frac{i\omega_{pi}^2\omega'}{\nu_i}\right]\left[c^2k_x^2 - \frac{ik_x^2V_e^2\omega_{pi}^2(\omega + i\nu_i)}{\omega\omega'\nu_i}\right] - \left[k_zk_xc^2 + \frac{i\omega_{pi}^2k_xV_e}{\nu_i}\right]\left[k_zk_xc^2 + \frac{i\omega_{pi}^2k_xV_e}{\nu_i}\left[1 - \frac{ik_zV_e\nu_i}{\omega\omega'}\right]\right], \tag{C9}$$

where $\omega' = \omega - k_zV_e$ and now $\omega = \omega_r + i\gamma$.

REFERENCES

1. P. F. Ottinger, D. Mosher and S. A. Goldstein, Phys. Fluids **22**, 332 (1979).

2. F. Sandel, G. Cooperstien, S. A. Goldstein, D. Mosher and S. J. Stephanakis, Bull. APS **23**, 816 (1978).

3. D. A. Hammer and N. Rostoker, Phys. Fluids **13**, 1831 (1970).

4. D. Mosher, D.G. Colombant, S.A. Goldstein and R. Lee, in *IEEE Conference Record-Abstracts, 1978 IEEE International Conference on Plasma Science, Monterey, California* (IEEE, New York, 1978) p. 113.

5. R. Lee and M. Lampe,. Phys. Rev. Lett. **31**, 1390 (1973).

6. K. Molvig, Phys. Rev. Lett. **35**, 1504 (1975).

7. S. A. Bludman, K. M. Watson and M. N. Rosenbluth, Phys. Fluids **3**, 747 (1960).

8. B. D. Fried and S. D. Conte, "The Plasma Dispersion Function" (Academic, New York, 1961).

9. G. Arfken, "Mathematical Methods for Physicists," 2nd ed. (Academic, New York, 1970) p. 474.

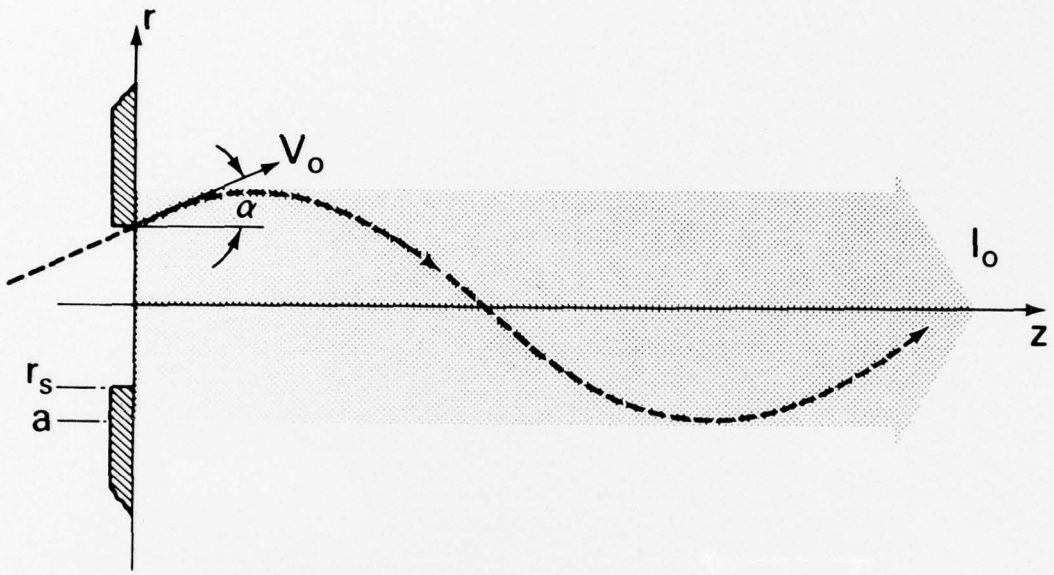

Figure 1 — Typical ion trajectory in the confining azimuthal magnetic field of the z-discharge channel after entering the channel from the focussing region on the left. Here V_0 is the speed of the beam ion, α in the injection angle, r_s is the spot size at injection and a is the channel radius.